Ferrimagnetic τ-MnAl/Co Superlattices on GaAs

G. Lauhoff,[1] C. Bruynseraede,[2] J. De Boeck,[2] W. Van Roy,[2,*] J. A. C. Bland,[1] and G. Borghs[2]
[1]*Cavendish Laboratory, Madingley Road, Cambridge CB3 OHE, United Kingdom*
[2]*IMEC, Kapeldreef 75, B-3001, Leuven, Belgium*
(Received 19 July 1996; revised manuscript received 27 May 1997)

We report on the ferrimagnetic superlattice ordering in epitaxial τ-MnAl/Co superlattices on GaAs. For ultrathin Co layers (3.5–7 Å), both the ferromagnetic τ MnAl and Co layers display a large perpendicular magnetic anisotropy together with an antiferromagnetic interface exchange coupling. As a result, an abrupt transition from the ferromagnetically aligned state at saturation to a ferrimagnetic superlattice ordering occurs at unusually high fields (3–7 T) followed by a reversal of the total sample moment at low fields (0.3–1.6 T). [S0031-9007(97)04893-X]

PACS numbers: 73.61.At, 75.70.Cn, 78.20.Ls

Magnetic superlattices (SL) are of substantial fundamental and applied interest since their properties can be significantly different from those of the component materials. A very wide range of magnetic SL has now been fabricated including SL of ferromagnetic (FM) with nonmagnetic (NM) layers (e.g., Ni/Mo [1], Fe/Si [2], Co/Ru [3]), FM with antiferromagnetic (AF) layers (e.g., Fe/Cr [4], Co/Mn [5]), AF with AF layers (e.g., Fe_3O_2/NiO [6]), or FM with FM layers. In this last category, direct exchange interactions at the interfaces occur leading to FM or AF coupling. FM interface coupling has been studied in a wide range of multilayers, e.g., Ni/Fe [7] and Ni/Co [8], but AF interface coupling is much rarer and has been reported in structures which include 4*d* series FM layers such as Fe/Gd and Co/Gd multilayers with small magnetic anisotropies and in-plane magnetization [9]. In this Letter, we describe the unusual exchange coupling and magnetic anisotropies in molecular-beam epitaxy (MBE) grown τ-MnAl/Co SL [10] observed by high field magneto-optic Kerr effect (MOKE) and extraordinary Hall effect (EHE) measurements. Earlier studies show that epitaxial τ-MnAl thin films are hard ferromagnets with perpendicular magnetic anisotropy (PMA) due to their epitaxial relationship with the underlying GaAs(001) substrate. This relationship forces the *c*-axis of the tetragonal τ-MnAl structure, which is the easy axis of magnetization, perpendicular to the film plane [11,12]. Here, we demonstrate for the first time that an AF coupling occurs at the τ-MnAl/Co interface, as previously predicted theoretically [13], which leads to a ferrimagnetic superlattice ordering [9] with perpendicular magnetization of the FM τ-MnAl and Co layer moments up to surprisingly high fields. Moreover, we show that an unusually abrupt magnetization reversal occurs at high fields due to the presence of a strong AF coupling in combination with a PMA in both constituent τ-MnAl and Co layers. This is in contrast to a more linear transition from the ferrimagnetic aligned state to the FM aligned state at saturation typically observed for Co/Gd or Fe/Gd SL with small anisotropies and in-plane magnetization [9].

The samples in this study are grown using a Riber 2300 molecular beam epitaxy system. Epitaxial growth of τ-MnAl/Co heterostructures includes the deposition of an AlAs buffer layer on GaAs(100) undoped substrates using standard conditions. This is followed by low temperature deposition of an amorphous template consisting of 2.5 monolayers $Mn_{60}Al_{40}$, a subsequent crystallization at about 250 °C, and finally the alternate deposition of τ-MnAl and Co layers at a substrate temperature of 220–250 °C. All samples were terminated by a τ-MnAl cap layer. *In situ* reflection high-energy electron diffraction monitoring together with transmission electron microscopy investigations and x-ray diffraction (XRD) analysis allow us to calibrate the metal deposition rates (0.6 ± 0.05 nm/min for Co and 1.7 ± 0.1 nm/min for τ-MnAl) and confirm the epitaxial relationship of the metal layers to the III-V substrate. Furthermore, they indicate a fourfold in-plane symmetry during the complete growth of the multilayers and reveal a close lattice matching between the τ-MnAl and Co epilayers. From these considerations, we expect the bcc Co phase to be the preferred growth mode for the ultrathin Co layers, which has been confirmed by XRD and nuclear magnetic resonance measurements [10,14]. The XRD data also reveal an excellent interface quality and confirm the SL nature of the τ-MnAl/Co heterostructures. More details about the growth and structural characteristics of these SL can be found elsewhere [10].

The polar MOKE and EHE measurements were performed at room temperature with a superconducting magnet [15]. Both polar MOKE and EHE measurements provide information on the magnetization component perpendicular to the sample. Figure 1 shows high field EHE data of three samples. The sample structures are given in Table I. For τ-MnAl/Co SL with thicker Co layers (8.5 Å, sample 1, curve *a*) we find that the Co layers have an in-plane and the τ-MnAl layers an out-of-plane remanent magnetization [10]. The observed hysteresis loop is a superposition of a square hysteresis loop at low fields attributed to the reversal of the τ-MnAl moments, and a

 0031-9007/97/79(26)/5290(4)$10.00

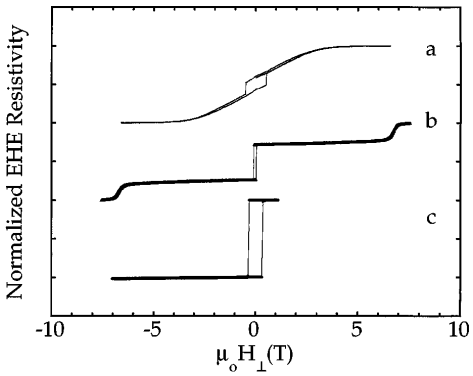

FIG. 1. EHE measurement with the field applied perpendicular to the film (curve *a*) of sample 1, (curve *b*) of sample 2, and (curve *c*) of sample 3. The loops are normalized to the saturation value of the EHE resistivity and shifted for comparison.

hard axis hysteresis loop attributed to the coherent rotation of the Co magnetization from an in-plane orientation at remanence to an out-of-plane orientation at saturation. In the case of the τ-MnAl/Co SL with ultrathin Co layers (4 Å, sample 2, curve *b*), a square loop at low fields is observed. Above the low switching field (50 mT) almost no change in the EHE signal is observed, indicating that no change in the amplitude of the perpendicular magnetization component occurs. But at an applied field of about 6.3 T an abrupt switching is observed, and at 7.5 T the sample is almost saturated. As a reference, EHE data for a single crystal 200 Å thick τ-MnAl film (sample 3) are given in curve *c* showing an almost square hysteresis loop with a coercive field of 0.3 T. The low field features of both curve *b* and curve *c* show a square hysteresis loop (with different coercive fields, however) which might indicate that the low field magnetization reversal for sample 2 (curve *b*) is determined by τ-MnAl. Both the absence of a hard axis hysteresis loop and the absence of an in-plane remanent magnetization for sample 2, as determined from in-plane alternating gradient field magnetometry (AGFM) measurements at low fields ($<$1.4 T), suggest that the Co magnetization is strongly coupled to the τ-MnAl magnetization which is perpendicular to the film surface. The observed high field switching as shown in curve *b* indicates that the τ-MnAl and Co layers are AF coupled to each other, resulting in Co and τ-MnAl spin orientations perpendicular to the sample surface. This ferrimagnetic superlattice ordering is maintained up to high fields and can only be broken for an applied field larger than 6.3 T.

TABLE I. Sample names and their structure descriptions.

Name	Sample structure	Shown in figure
Sample 1	6× {τ-MnAl(36 Å/Co(8.5 Å)}	Fig. 1(a); Fig. 2(a)
Sample 2	6× {τ-MnAl(18.5 Å/Co(4 Å)}	Fig. 1(b); Fig. 4
Sample 3	200 Å τ-$Mn_{60}Al_{40}$	Fig. 1(c)
Sample 4	6× {τ-MnAl(20 Å/Co(5 Å)}	Fig. 2(b)
Sample 5	6× {τ-MnAl(20 Å/Co(3–7 Å)}	Figs. 3(a)–3(e)

Other possible explanations for the observed high field features can be ruled out. First, a biquadratic coupling between the τ-MnAl and the Co layers could lead to similar high field behavior. But in this case, an in-plane remanent magnetization should be observed. AGFM measurements show that this is not the case and therefore exclude this possibility. Second, structural disorder in the τ-MnAl unit cell affects the magnetic properties of this alloy in the sense that the ideal stacking of Mn and Al on alternating planes of the tetragonal lattice is no longer achieved, leading to an AF coupling between Mn atoms on Mn sites and Mn atoms on Al sites [11,12]. These antiferromagnetically aligned Mn atoms in the crystal lattice could then also experience a spin reversal at high fields. This mechanism, however, should also be present in single τ-MnAl thin films, grown in otherwise identical conditions, but was never detected, as shown in Fig. 1(c). Furthermore, theoretical predictions by Van Leuken and de Groot [13] indicate that a coupling between τ-MnAl and Co layers would be AF for a Mn terminated interface between the τ-MnAl and Co layers, supporting our conclusion of AF coupling.

Polar MOKE measurements on various SL corroborate the AF coupling model and will allow us to evaluate which of the two sublayers is switching at high fields. From MOKE measurements on sample 1, given in Fig. 2 (curve *a*), we conclude that the τ-MnAl and Co layers have the same sign of Kerr rotation. With this information, a clear AF coupling between the two constituent layers of sample 4 can be identified from the data of Fig. 2

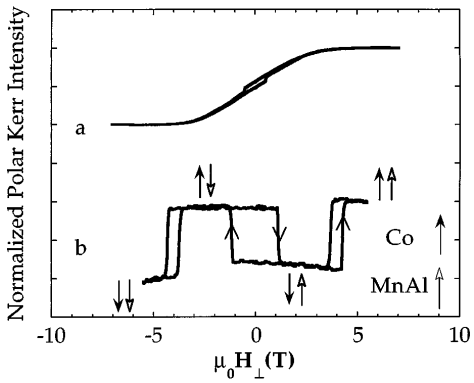

FIG. 2. Polar MOKE measurement with the field applied perpendicular to the film (curve *a*) of sample 1 and (curve *b*) of sample 4. The loops are normalized to the saturation intensity and shifted for comparison. The direction of the Co and τ-MnAl magnetizations at remanence and at saturation, as discussed further in the paper, are added for clarity. A linear background has been subtracted.

(curve *b*). At the low field reversal (at 1 T), the MOKE intensity drops, when ramping up the field. This can only occur when the magnetic moments of the τ-MnAl and Co layers switch simultaneously, remaining strongly AF coupled, and the MOKE contribution from the subset of layers forced antiparallel to the applied field is largest. At higher fields the AF coupling between Co and τ-MnAl is broken and the Kerr intensity rises as the magnetization directions become aligned.

In order to identify which subset of layers is switching at high fields, the influence of the thickness of the Co layers on the AF coupling in these τ-MnAl/Co SL was studied. A special wedged $6\times$ {τ-MnAl(20 Å)/Co(3–7 Å)} SL (sample 5) was grown for this purpose [16]. Three typical polar MOKE loops of the wedge are shown in Figs. 3(a)–3(c). Very sharp switching is observed both at high and low fields. Curve *d* shows the Co thickness dependent field values, at which the AF coupling between the Co and τ-MnAl is broken when ramping up the field, whereas curve *e* gives the field values at which the magnetizations for Co and τ-MnAl switch back to the AF orientation. These data clearly show a lower saturation field for thicker Co layers, indicating that it is the Co layers which are switching to the FM orientation at high fields.

We have modeled numerically the magnetization process of the τ-MnAl/Co SL in order to estimate the AF coupling strength and the possible presence of a PMA in the Co layers using an energy minimization approach [17]. We use the bulk magnetization for τ-MnAl (490 kA/m) [12] and fcc Co (1420 kA/m) and a magnetocrystalline anisotropy constant for τ-MnAl of $K_{\mathrm{MnAl}} = 2\ \mathrm{MJ/m^3}$ [18]. Both the exchange coupling strength (J_1) and PMA for Co are fitted numerically to the observed magnetization loops. For sample 2 in Fig. 4(b) an AF coupling strength of $J_1 = -1.9\ \mathrm{mJ/m^2}$ per interface has been extracted. The field range in which the magnetization reversal of the Co layers at high field occurs would become progressively larger as the PMA for Co is decreased, as can be seen in Fig. 4 (compare curve *b* with curve *c*). A large effective PMA for Co of $K_{\mathrm{eff}}(\mathrm{Co}) = 1.2\ \mathrm{MJ/m^3}$ has therefore been extracted. While more accurate values for the magnetizations of Co and τ-MnAl are required for a precise determination of the coupling strength and Co PMA, we can nonetheless conclude from our simulations that the ratio of J_1/M_{Co} does not change significantly over a wide range of values for M_{MnAl} and M_{Co} and that a PMA for *both* τ-MnAl and Co must always be present.

The same energy minimization approach also enabled us to model the Co thickness dependent saturation field (Fig. 3 lower figure) assuming a slightly reduced magnetization for the Co layers of 1100 kA/m, yielding an effective PMA for Co of $K_{\mathrm{eff}} = 0.5\ \mathrm{MJ/m^3}$ and a constant exchange coupling strength $J_1 = -1.15\ \mathrm{mJ/m^2}$, which confirms the interfacial origin of the AF coupling between τ-MnAl and Co. Moreover, it was only possible to fit these Co thickness dependent M-H loops with a constant value for J_1 by assuming a smaller total magnetic moment for the Co layers than for the τ-MnAl layers. This leads us to the conclusion that it is indeed the Co layers which are abruptly switching at high fields. The increase in the low field τ-MnAl coercivity with increasing Co layer

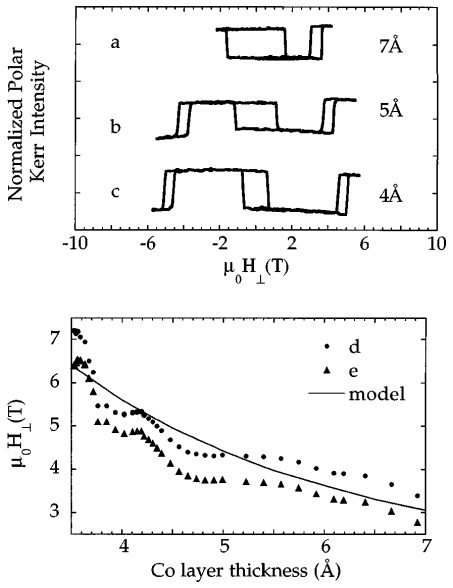

FIG. 3. (upper figure) Polar MOKE measurements with the field applied perpendicular to the surface of the wedged SL (sample 5). The nominal Co layer thicknesses are 7 Å (curve *a*), 5 Å (curve *b*), and 4 Å (curve *c*). The loops are normalized to the saturation value and shifted for comparison. A linear background has been subtracted. (lower figure) Curve *d* shows the field values, at which a sharp magnetization reversal is observed at high field when ramping up the field, and curve *e* shows the corresponding field values when ramping down. The Co thickness dependent saturation field can be modeled as indicated in the figure (continuous line) using $J_1 = -1.15\ \mathrm{mJ/m^2}$ and $K_{\mathrm{eff}}(\mathrm{Co}) = 0.5\ \mathrm{MJ/m^3}$.

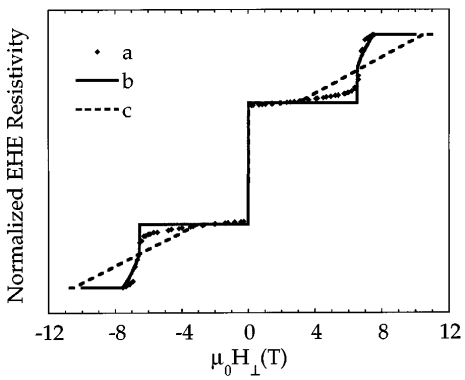

FIG. 4. (curve *a*) EHE measurement of sample 2 (normalized to saturation value). (curve *b*) A modeled M-H loop for $J_1 = -1.9\ \mathrm{mJ/m^2}$ and $K_{\mathrm{eff}}(\mathrm{Co}) = 1.2\ \mathrm{MJ/m^3}$. Note that for a smaller $K_{\mathrm{eff}}(\mathrm{Co})$ the Co moment switches less abruptly at high fields as shown in (curve *c*) using $J = -1.9\ \mathrm{mJ/m^2}$ and $K_{\mathrm{eff}}(\mathrm{Co}) = -2\pi M_{\mathrm{Co}}^2 = -1.3\ \mathrm{MJ/m^3}$, which includes only the shape anisotropy of Co.

thicknesses (0.3 to 1.6 T) as shown in Figs. 3(a)–3(c) can be ascribed to structural changes in the SL. Thicker Co layers might lead to rougher interfaces and therefore an increased number of pinning sites for the τ-MnAl magnetization reversal process. For films with Co thicknesses below 3.5 Å, we find a loss of AF coupling which we attribute to the breaking of the SL structure and an evolution to a τ-MnAlCo alloy as indicated by XRD measurements.

In summary, we have shown that τ-MnAl/Co SL epitaxially grown on GaAs(001) show a strong AF interface exchange coupling combined with a large PMA for *both* the τ-MnAl and ultrathin Co layers (3.5–7 Å). This results in an unusually abrupt spin reversal at high fields, observed by EHE and polar MOKE measurements. From the polar MOKE measurements of a SL with wedged Co interlayers it is conclusively shown that the observed magnetization reversal at high field can be attributed to the Co spin reversal from the antiparallel to the parallel orientation with respect to the magnetization of the τ-MnAl layers. Our work illustrates how the presence of additional magnetic anisotropies together with AF interlayer coupling can lead to new spin reversal processes.

The authors thank Robert Hicken for valuable discussions. The authors acknowledge the financial support of the EPSRC (U.K.), the Newton Trust (U.K.), the EU under Grant No. ESPRIT 20.027, the IWT (Flanders, Belgium), and the National Fund of Scientific Research (Belgium).

*Present address: Joint Research Center for Atom Technology-Angstrom Technology Partnership, 1-1-4 Higashi, Tsukuba, Ibaraki 305, Japan.

[1] M. Grimsditch *et al.*, Phys. Rev. Lett. **51**, 489 (1983).
[2] C. Dufor *et al.*, J. Magn. Magn. Mater. **93**, 545 (1991).
[3] S. S. P. Parkin, N. More, and K. P. Roche, Phys. Rev. Lett. **64**, 2304 (1990).
[4] P. Grünberg *et al.*, Phys. Rev. Lett. **57**, 2442 (1986).
[5] Y. Henry and K. Ounadjela, Phys. Rev. Lett. **76**, 1944 (1996); K. Uchiyama *et al.*, J. Magn. Magn. Mater. **156**, 429 (1996); A. Michel *et al.*, J. Magn. Magn. Mater. **156**, 23 (1996).
[6] C. A. Ramos *et al.*, Phys. Rev. Lett. **65**, 2913 (1990).
[7] W. L. O'Brian and B. P. Tonner, Phys. Rev. B **52**, 15 332 (1995).
[8] G. H. O. Dalderop, P. J. Kelly, and F. J. A. den Broeder, Phys. Rev. Lett. **68**, 682 (1992).
[9] Y. Kamiguchi, Y. Hayakawa, and H. Fujimori, Appl. Phys. Lett. **55**, 1918 (1989); R. E. Camley and D. R. Tilley, Phys. Rev. B **37**, 3413 (1988).
[10] J. De Boeck *et al.*, J. Cryst. Growth **150**, 1139 (1995); C. Bruynseraede *et al.*, Mater. Res. Soc. Symp. Proc. **384**, 85 (1995).
[11] T. Sands *et al.*, Appl. Phys. Lett. **57**, 2609 (1990); W. Van Roy *et al.*, J. Appl. Phys. **78**, 398 (1995).
[12] A. J. J. Koch *et al.*, J. Appl. Phys. **31**, 75s (1960).
[13] H. van Leuken and R. A. de Groot (private communication); H. van Leuken *et al.*, Phys. Rev. B **41**, 5613 (1990).
[14] G. Strijkers and H. Swagten (private communication).
[15] A. J. R. Ives *et al.*, J. Appl. Phys. **75**, 6458 (1994).
[16] C. Bruynseraede *et al.* (to be published).
[17] B. Dieny, J. P. Gavigan, and J. P. Rebouillat, J. Phys. Condens. Matter **2**, 159 (1990); B. Dieny and J. P. Gavigan, J. Phys. Condens. Matter **2**, 187 (1990).
[18] The *c*-lattice constant obtained from XRD measurements is 3.38 Å. For this constant, $K_{\mathrm{MnAl}} = 2\ \mathrm{MJ/m^3}$ is expected after A. Sakuma, J. Phys. Soc. Jpn. **63**, 1422 (1994).